Mobility measurements of two kinds of two-dimensional fluids. Methane adsorbed on graphite

J.P. Coulomb, M. Bienfait, P. Thorel

J. Physique **42** (1981) 293-306 FÉVRIER **1981**, PAGE 293

Classification
Physics Abstracts
68.15 — 64.70F

Mobility measurements of two kinds of two-dimensional fluids. Methane adsorbed on graphite (*)

J. P. Coulomb, M. Bienfait (**)

Faculté des Sciences de Luminy, Département de Physique, 13288 Marseille Cedex 2, France

and P. Thorel

C.E.N.G., D.R.F., Physique du Solide, 85X, 38041 Grenoble Cedex, France

(*Reçu le 5 septembre 1980, accepté le 6 octobre 1980*)

Résumé. — Le coefficient de diffusion d'une couche de CH_4 adsorbée sur la face (0001) du graphite est mesuré par diffusion quasi élastique de neutrons, en fonction du degré de recouvrement et de la température. Les données expérimentales permettent de différencier nettement deux types de fluides adsorbés : un liquide bidimensionnel coexistant avec un gaz et un fluide hypercritique dont la densité varie continuement avec le degré de recouvrement. La mobilité disparaît à la solidification qui peut être obtenue par diminution de la température à degré de recouvrement constant ou par augmentation de la concentration à constante température. La coexistence du solide et du liquide bidimensionnels a aussi été observée. Enfin, tous ces résultats sont utilisés pour tracer un diagramme de phase de la première couche de méthane adsorbée sur le graphite.

Abstract. — The diffusion coefficient of a CH_4 submonolayer adsorbed on (0001) graphite is measured as a function of coverage and temperature by quasi-elastic neutron scattering. The experimental data permit us to clearly distinguish two kinds of adsorbed fluids, i.e. a 2D liquid coexisting with a 2D gas and a 2D hypercritical fluid whose density varies continuously with coverage. The mobility disappears at solidification which can be obtained either by decreasing temperature at constant coverage or by increasing coverage at constant temperature. The coexistence of 2D solid and 2D liquid is also observed. Finally a phase diagram of the first layer of methane adsorbed on graphite is proposed.

1. **Introduction.** — Monolayers physisorbed on well defined cleavage faces of crystals are a good representation of a two-dimensional (2D) world despite the influence of the adsorption potential of the substrate. This potential has its own periodicity and compels us to consider forces different from the lateral interactions of the layer neighbours. The adsorbed monolayers exhibit different phases which have been inferred by adsorption isotherm measurements [1]. The transitions between these phases raised a great interest in the scientific community due to their quasi two-dimensional behaviour. The characterization of these phases has been achieved during the last few years by thermodynamic techniques (adsorption isotherm measurements, calorimetry), diffraction studies (LEED, neutron, X-rays) or molecular dynamics as well (NMR, QENS). Several recent books and review papers made a critical analysis of the knowledge in the field [2-6]. Although 2D matter begins to be comprehended, numerous questions are still open.

Of principal interest is the nature of the various fluids expected to be stable on surface films. Some theoreticians proposed a melting of 2D solids through a two-step process [7, 8]. A *floating solid* or *hexatic phase* with persistence of a long range orientational order should appear before an isotropic 2D liquid. Both transitions solid-*floating solid*-isotropic liquid should be continuous. Very recently, these views seem to have been confirmed experimentally for helium submonolayers [9]. However those predictions were questioned by other theorists [10-12] who claimed that melting is a first order transition, i.e. 2D isotropic liquid occurs suddenly at melting. An experimental verification of these predictions for methane films was published a few months ago [13].

If 2D melting is a first order transition, one can expect, as in bulk matter, to observe two kinds of dense fluids [1, 2]. One, called 2D liquid, is stable

(*) Experiment performed at « Institut Laue-Langevin ».
(**) Equipe de Recherche Associée au C.N.R.S. 899.

between a 2D triple point and a 2D critical temperature and has a very narrow existence domain in density. A change of density (coverage) yields to a coexistence with a solid (increasing density) or with a gas (decreasing density). This liquid cannot cover the whole surface offered to it. Distinct from this fluid, if $T > T_c$, a so-called hypercritical fluid, highly compressible, covers the whole available surface till the density is high enough to solidify.

The results reported here favour the latter views for methane films adsorbed on graphite. We confirm the first order melting transition of a submonolayer of this simple hydrocarbon and perform a careful analysis of the 2D fluids below and above the 2D critical temperature. We show that the 2D liquid-gas transition is also of first order below the 2D critical temperature.

Neutron diffraction which measures the coherence length of the condensed phases can answer the question of the melting transition [13] but is unable to settle the problem of different types of liquids. This is the reason why we chose quasi-elastic neutron scattering (QENS). This technique usually yields mobility measurements. Our feeling was that this mobility should be very sensitive to the local density. In the case of a *true* liquid which forms two-dimensional islands in equilibrium with another phase (solid or gas), the local density is constant as the coverage changes. As for the hypercritical fluid, the local density varies inversely with coverage, leading to mobility changes. Note these neutron probe techniques are not sensitive enough to detect a signal coming from the 2D gas which is a too dilute phase.

On the other hand, the mobility of 2D fluids received attention from theorists [14, 15] who wondered whether the diffusion coefficient would diverge in two dimensions. A measurement of mobility as a function of coverage will probably stimulate the debate on the long-time behaviour of the velocity autocorrelation function.

Preliminary reports were published some time ago [16, 17]. In order to deal with this problem, we measured the mobility of a submonolayer of methane physisorbed on graphite and its variation as a function of coverage and temperature. The 2D melting is demonstrated by an abrupt increase of the mobility of the admolecules when going from the solid-gas coexistence domain to the liquid-gas coexistence domain. This increase can be seen not only by QENS but also by NMR [9, 18-21, 37] and Mössbauer spectroscopy as well [22]. These three nuclear techniques are sensitive only to very few types of nuclei which must be incorporated into the admolecules. QENS is restricted to ^1H nuclei due to their strong incoherent scattering cross-section. But it is sufficient to open the field of the organic molecules.

Among the three techniques, QENS seemed to be the more efficient as it can show evidence of the two expected different condensed fluids. This paper is a detailed report on our findings.

We chose the system methane on graphite because the molecule was simple, spherical at the temperature of the experiment ($T > 50$ K) and its interaction potential with the cleavage face of graphite was well known. So it is easy to build 2D models e.g. lattice gas [23-25] or molecular dynamics [26-28]. This system is very similar to the rare gases on graphite where a strong theoretical effort and a lot of computer simulations were recently reported [3, 29-34]. For these reasons, it is a typical case of 2D adsorbed phases.

Moreover this system is approachable through different complementary techniques : adsorption isotherms [1, 35, 36], NMR [18, 37], QENS [16, 17, 38, 39] and neutron diffraction of the deuterated compound [13, 40, 41]. Its thermodynamic properties are fairly well known [1] above 77 K. The 2D-critical temperature is estimated around 75 K, while neutron diffraction yields a triple point at 56 K. The liquid-gas coexistence domain spreads out within 20 K, so it allows an easy characterization of its properties.

2. **Adsorption and quasi-elastic neutron scattering.** —

2.1 PAPYEX ADSORBING PROPERTIES. — The substrate is a recompressed exfoliated graphite called papyex with properties similar to grafoil [2, 6]. Its important volumic adsorption area (~ 20 m^2/cm^3), mainly made of basal plane (0001) surfaces, shows little variation depending on adsorbate and outgasing procedures. This industrial product is suitable for neutron scattering studies on two-dimensional phases. Although it had been intensively used [13, 16, 17], it remained incompletely characterized. Up to the present it has been assumed that the orientation distribution of papyex is the same as that of grafoil, although no characterization had been made of papyex specifically. As a matter of fact, papyex exhibits a preferred alignment of the basal planes parallel to the plane of the foil, with a distribution similar to that of grafoil.

We present here a careful determination of the probability density $g(\beta)$ of the crystallite surfaces, i.e. the angular distribution of the (0001) adsorbing area, with respect to the normal of the foil. The function is obtained from diffraction experiments (see appendix) and is drawn in figure 1. The distribution is isotropic around the normal of the foil plane and has a full width at half maximum of about 30°. This partial orientation allows the use of geometrical selection rules relating the direction of molecular motions to the scattering vector direction. For instance, an in-plane geometry (i.e. a configuration where the neutron scattering plane is parallel to the mean orientation of the graphite basal planes), emphasizes the molecular movement components along the (0001) surfaces. We shall come back on this important point in 2.2.

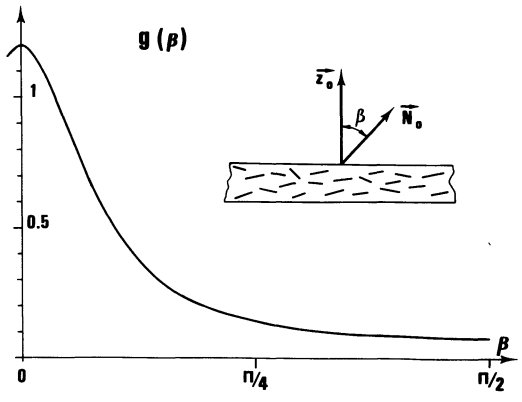

Fig. 1. — Orientational distribution $g(\beta)$ of the (0001) adsorbing area. $g(\beta)$ obeys equation (A.1) with $q = 0.6$.

Adsorption isotherm measurements of CH_4 on papyex were performed after an outgasing under vacuum at 400 °C for 6 hours. They exhibit the well-known steps characteristic of the classical two-dimensional transitions [1] occurring in the adsorbed first atomic layer. The detailed study was reported previously [16]. It confirms that papyex has a well-defined uniform surface and is a substrate well adapted for two-dimensional phase analysis.

The neutron scattering cell is filled up with a stack of outgased papyex discs and set in a liquid helium cooled cryostat. The calibration of the methane amount adsorbed on the 55 g of papyex is carried out in this experimental set-up prior to neutron scattering measurements [16] by recording an adsorption isotherm. Figure 2 represents schematically the experimental arrangement together with the obtained adsorption isotherm. The coverage $x = 1$ is defined

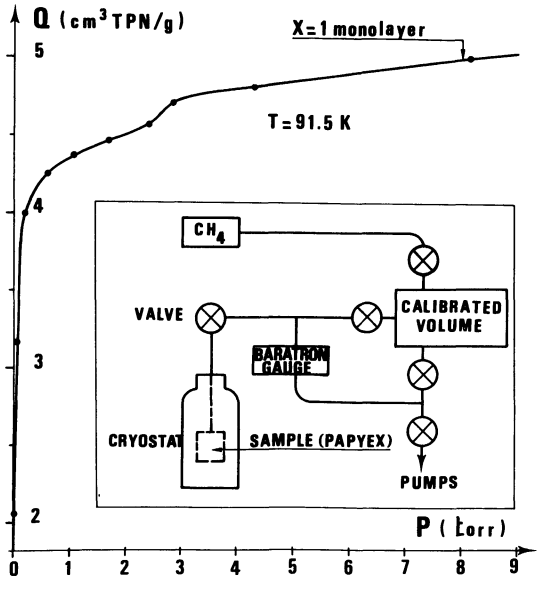

Fig. 2. — Adsorption isotherm at 91.5 K of CH_4 on papyex measured in the experimental set-up drawn in the box. The small substep represents the fluid-solid transition. The monolayer completion ($x = 1$) corresponds to 5 cm³ TPN/g and to a molecular density of 0.073 Å^{-2}.

by the inflexion point on the plateau of the isotherm between the first and second layer (usually called point B_1 by physical-chemists). From our adsorption isotherm measurements, it corresponds to a surface density of about 0.07 Å^{-2}. The detailed structural analysis by Vora *et al.* [41] permits one to define precisely the monolayer completion of the compressed structure, i.e. 0.073 Å^{-2}. Here we accept this coverage calibration.

2.2 NEUTRON SPECTROSCOPY. — All the measurements were made on the time-of-flight spectrometer IN5 at ILL using a fixed incident neutron wavelength λ. Several runs were carried out either at $\lambda = 6.0$ Å ($E_0 = 2.27$ meV) or at $\lambda = 8.0$ Å ($E_0 = 1.28$ meV). The instrumental resolution was 80 μeV and 35 μeV respectively. The wavelengths were larger than the cut-off wavelength of the $hk.0$ diffracted graphite beams. The quasi-elastic incoherent spectra were recorded for various values of the wavevector **Q** ranging from 0.18 to 1.93 Å^{-1} and converted into the scattering cross-section $S''(Q, E)$ without correcting for instrumental resolution.

2.3 TRANSLATIONAL MOBILITY. — 2.3.1 *Quasi-elastic neutron scattering by* 3D *liquids.* — The theory of quasi-elastic neutron scattering by three-dimensional liquids has been established a few years ago and can be found in standard books dealing with formalism of neutron scattering. Readers not familiar with this topic, can refer for instance to the review paper by S. Springer [42] or to the book of Marshall and Lovesey [43]. Neutrons can exchange momentum and energy with moving molecules. Hence a monochromatic incident beam interacts with the molecules of a liquid and is scattered quasi-elastically. On a microscopic scale, the molecular movements are described by the pair correlation functions according to the representation of Van Hove [44, 45].

As the methane molecule has a strong incoherent cross-section (320 barns) we have access only to the self correlation function i.e. the information concerning the individual molecular motions. We can take into account three kinds of movements : translation (centre of mass motion), rotation (overall rotation of the molecule around the centre of mass) and vibration, i.e. high frequency motion around the mean translation path or intramolecular vibration. If we have no coupling between these motions, the theoretical treatment leads to the following results. The molecular translational and rotational motions yield a Doppler broadening of the line. In our case, the methane molecule rotates so quickly

$$(\omega_r \simeq 10^{13}\ \text{rad.s}^{-1})$$

that it does not contribute to any extra broadening of the quasi-elastic spectra. So we can take into account the translational diffusion only. With the usual instrumental resolution (35 or 80 μeV), the

time scale t (10^{-9} s) of the probe is larger than the relaxation time of the liquid τ_0 and the long-time behaviour of the correlation function is observed. Assuming that the self correlation function obeys the Fick equation of diffusion, the motional broadening has a Lorentzian shape at small scattering vector **Q**. The scattering law $S(\mathbf{Q}, \mathbf{E})$ has the simple form

$$S(\mathbf{Q}, \mathbf{E}) = \frac{F(\mathbf{Q})}{\pi} e^{-Q^2\langle u^2\rangle} \frac{\hbar DQ^2}{(\hbar DQ^2)^2 + (E - E_0)^2} \quad (1)$$

where E_0 and E are the incident and scattered energy respectively, D is the translational diffusion coefficient and $F(\mathbf{Q})$ [46] is the elastic incoherent structure factor (EISF). The term $e^{-Q^2\langle u^2\rangle}$ accounts for high frequency motions and is similar to the Debye-Waller factor well-known in diffraction theory.

In fact it is possible to build more sophisticated models involving a jump time τ between preferential sites (distance l), and residence time on each site [47], but all these models yield the same asymptotic behaviour for low Q which allows the definition of such a macroscopic D coefficients $\left(D \sim \frac{\langle l^2 \rangle}{4\tau}\right)$. In any case the physical information on the nature of the fluid we are interested in is all enclosed within this macroscopic D and is sufficient to find the extension of the liquid-gas coexistence domain.

2.3.2 *Quasi-elastic neutron scattering by 2D fluids.* — This formalism has been able to interpret successfully the translational mobility of simple three-dimensional liquid but one can wonder whether it accounts for diffusion in surface films. Two difficulties compel recognition. First the substrate brings an important contribution to neutron scattering. It can, in principle, be easily removed by subtracting the bare spectra due to graphite from the scattered line due to graphite plus surface layer.

This process introduces a small perturbation near $E = E_0$ because the incident beam is slightly attenuated by the overlayer. A small drop having the instrumental resolution near E_0 is often observed in the difference spectra (see for instance Fig. 3). This is the so-called self shielding effect. It can be left out of account for the quantitative interpretation. The second difficulty is more serious. It has been recognized that a powder of disorientated planes scatters neutrons according to a law different from equation (1) [48, 49]. Let us consider a surface bearing a 2D fluid and making an angle τ with the scattering vector **Q** (τ is the angle between the normal $\mathbf{N}_0$ to the plane and **Q**). The 2D fluid is restricted to move along the surface and equation (1) becomes

$$S_\tau(\mathbf{Q}, \mathbf{E}) = \frac{F(\mathbf{Q})}{\pi} e^{-Q^2\langle u^2\rangle} \frac{\hbar DQ^2 \sin^2\tau}{(\hbar DQ^2 \sin^2\tau)^2 + (E - E_0)^2}. \quad (2)$$

This means that if $\tau = 0$, i.e. if **Q** is perpendicular to the surface, the broadening collapses and the 2D fluid cannot be detected anymore. This geometry is not appropriate to measure 2D mobility. Conversely the in-plane geometry ($\tau = \pi/2$) yields the right diffusion measurement. An actual powder mixes the two configurations but the texture of papyex allows a configuration close to the in-plane geometry. In our preliminary reports, we interpreted the observed broadenings according equation (1). All the experimental data were correctly fitted by Lorentzian lines where ΔE (full width at half maximum) was taken equal to $2\hbar DQ^2$ and we attributed this good agreement to the preferential orientation of graphite crystallites in papyex.

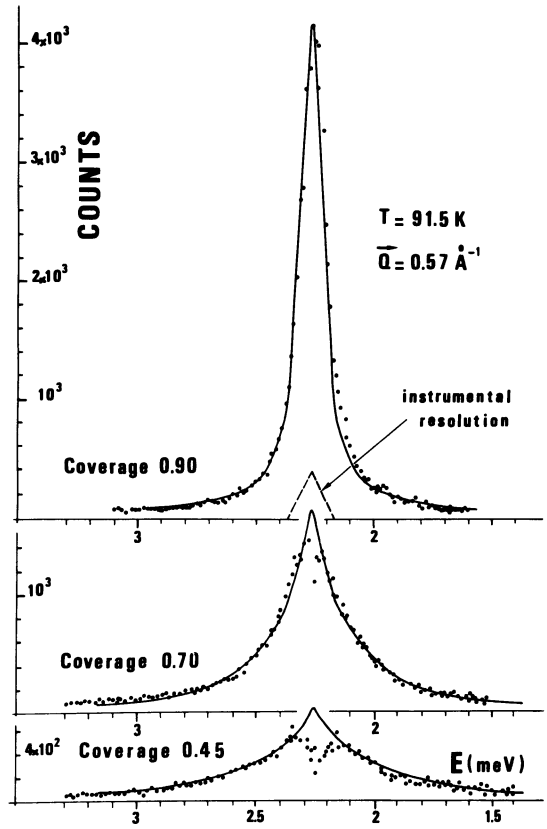

Fig. 3. — Quasi-elastic difference spectra of CH_4 submonolayers adsorbed on graphite. Broadening i.e. mobility increases when coverage decreases. Typical background level (bare graphite spectra) is 2×10^3 counts for E_0 the neutron incident energy. All the spectra are normalized to the same incident flux. The full lines represent the best fit with equation (3) ($D = 3.5, 13, 22 \times 10^{-5}$ cm^2.s^{-1} respectively). The central dip in the 0.45 curve is due to self shielding effect.

In this more detailed paper, we will analyse the influence of disorientated crystallites on the shape of the scattering law. Expression (2) must be integrated over all the distribution of the adsorbing planes :

$$S'(\mathbf{Q}, E) = \int_0^{2\pi} \int_0^{\pi} S_\tau(\mathbf{Q}, E)\, g(\beta) \sin\tau \, d\tau \, d\eta . \quad (3)$$

The notation and complete demonstration are given in Appendix. As a result, it comes that the perturba-

tion due to misorientation is not negligible. The scattering law is no longer Lorentzian and now diverges at $E = E_0$. Nevertheless, if we take into account the instrumental resolution, a Lorentzian shape is approximately recovered except in the resolution domain near E_0 which is already polluted by self shielding.

As all the fits of the previous papers were performed on the whole curve except around E_0, it is easy to understand why we could use expression (1) to fit the experimental results although we are now aware of having to employ equation (3) to reduce the data. Unfortunately the value of D which allows to fit the experimental curves is not the same when using expressions (1) or (3). Computations show in the case of papyex that the ratio $\frac{D(3)}{D(1)}$ between the diffusion coefficient obtained with equations (3) and (1) respectively is about 1.7 and does not depend on Q. As a consequence, we must change our previous scale of D and multiply the values given in [16, 17, 38, 50] by a factor 1.7. This correction does not modify qualitatively the conclusions obtained previously because they were based on the relative variation of D with temperature and coverage.

2.4 LINE SHAPE AND WIDTH. — 2.4.1 *Out-of-plane geometry.* — The major parts of the experiments were performed in the in-plane geometry ($\tau = \pi/2$), but one of them was carried out in the out-of-plane arrangement ($\tau = 0$). It is reported in the Appendix. If all the graphite crystallites in papyex were perfectly aligned in the out-of-plane geometry, we should see no broadening at all as explained above. Neutrons would only probe the mobility in the direction perpendicular to the layer. Although there are some exchanges between the vapour phase surrounding the crystal and the surface films, the major part of the molecules are restricted to move within the adsorbed layer. The average mobility in the direction normal to the surface film is nearly zero. In fact, the small broadening observed in the quasi-elastic spectra (Fig. 13*b*, Appendix) is perfectly explained by the misorientated crystallites according to equation (3).

2.4.2 *In-plane geometry.* — Three difference spectra measured in the in-plane geometry configuration are represented in figure 3 at constant temperature (91.5 K) and wavevector (0.57 $Å^{-1}$) for different coverages. The full width at half maximum is clearly larger than the instrumental resolution indicating a movement of the CH_4 molecules inside the adsorbed layer. The full lines are given by equation (3) convoluted by the instrumental resolution. They are obtained as the best fit of a computation where two parameters, the peak intensity (see eq. (2)) and D (responsible for the broadening) are adjusted. The good agreement between these experiments and theory is a good test for the validity of equation (3).

Figure 4 represents the diffusion coefficient D as a function of Q at constant temperature T and coverage x. The constant value of D up to $Q = 1.4$ $Å^{-1}$ for $x = 0.9$ and 0.7 shows that the condition *small Q* is always fulfilled in those experiments. However for $x = 0.45$, the experimental D is no longer constant above ≈ 1 $Å^{-1}$. In this case equation (3) should take into account more sophisticated models.

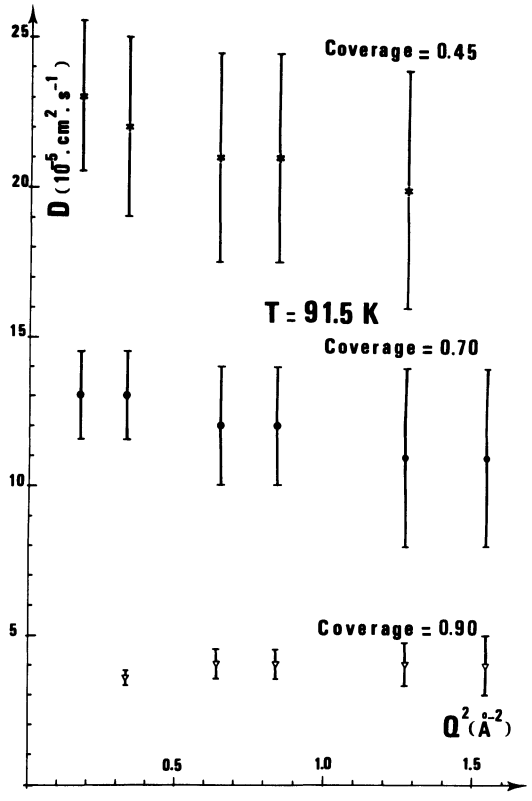

Fig. 4. — Diffusion coefficient *versus* square of the scattering vector for different coverages.

The broadening disappears when the layer is solidified. This can be obtained in two ways either by increasing coverage up to $x = 1$ at constant temperature (1) or by cooling down a submonolayer ($x < 1$) below the triple point at 56 K. These points will be developed in 3.1 and 3.2. They are quoted here to emphasize once more that the observed broadening of the quasi-elastic line indicates that we do measure the mobility of the CH_4 molecules.

Several quasi-elastic spectra obtained in various coverage, temperature and wavevector conditions have been published so far [16, 17, 38, 50]. We do not want to duplicate them here. We will just report the measurements of the 2D diffusion coefficients obtained in various physical conditions and draw a conclusion about the various kinds of 2D fluids and about their mutual coexistence or their coexistence with a solid phase.

3. **Results and interpretation.** — 3.1 HYPERCRITICAL FLUID. — Above the 2D critical temperature

(~ 75 K), the fluid is called *hypercritical phase* [1] and should correspond to the three-dimensional gas stable above T_c(3D). Its mobility has been measured and partly reported in a preliminary paper [16]. In table I, we give a complete set of our measurements (with D corrected as previously mentioned in 2.3.2).

Table I. — *Diffusion coefficient in* 10^{-5} $cm^2.s^{-1}$ *of the* 2D *hypercritical fluid* versus *coverage and temperature. D is coverage dependent.*

x	81.5 K	91.5 K	101.5 K
0.45		22 ± 4	
0.70		12 ± 2	
0.72	10 ± 2	11.5 ± 2	12 ± 2
0.90	3.2 ± 1.0	4.0 ± 0.5	6.3 ± 0.5

The salient result is the important variation of D with coverage at constant temperature. For $x > 1$ and $T = 91.5$ K [16], D is zero within the limit of the experimental uncertainty. The layer is solidified as expected from the adsorption isotherm measurements [1]. A reproducibility experiment was performed at 91.5 K and $x = 0.70$; the value found for D was 12×10^{-5} $cm^2.s^{-1}$ in good agreement with the diffusion coefficient measured at $x = 0.72$ for the same temperature (11.5×10^{-5} $cm^2.s^{-1}$).

The variation of D with T at constant coverage (i.e. constant density) means that translational diffusion is an activated process. The few explored temperatures yield only an estimate of such an activation energy of diffusion; its value is 7 meV (150 $cal.mole^{-1}$) and 22 meV (500 $cal.mole^{-1}$) for $x = 0.7$ and 0.9 respectively. Both activation energies have been calculated using the central values of D listed in table I and they are known with a large uncertainty. However they are definitely different. This indicates a strong influence of the CH_4 lateral interactions on the diffusion process. These energies have to be compared to the depth of the graphite surface potential wells (≃ 12 meV) [51]. A more detailed study should be performed to draw more precise conclusions on this thermal activated process.

On the other hand, the strong variation of D with x at fixed T is more striking, especially at 91.5 K. The drastic decrease of D when x is raised can be explained qualitatively by an increase of the fluid density with coverage. The free space between moving molecules is reduced resulting in a mobility drop. Two quantitative explanations have been proposed.

We imagined a simple cell model where the fluidity was proportional to the number of holes in the adsorbed layer, i.e. to the free area [16]. This idea is the transposition in two dimensions of the model of Eyring [52] commonly used to interpret the mobility of bulk liquid. Then the translational diffusion coefficient is a function of coverage

$$D \sim (1 - x)/x^{1/2} .$$

This relation is approximately verified by the experimental data [16].

The other explanation deals with a molecular dynamics simulation of the mobile layer [26]. The methane film is modelled by a Lennard-Jones ensemble. The computation gives a value of D at high coverage in reasonable agreement with the experiment. Furthermore the calculation can be carried out with or without an external potential (the graphite field). The results show that the diffusion coefficient is only slightly modified by the substrate potential, a conclusion indicating that the mobile layer is very close to an ideal two-dimensional fluid.

3.2 LIQUID-GAS COEXISTENCE DOMAIN. — As pointed out before, QENS is unable to get any information from the 2D-gas phase which is not dense enough and much too mobile and yields a very flat and broad spectrum which may be taken as a flat background. Hence the only detectable information comes from the dense phase.

3.2.1 *Changing coverage at constant temperature.* — These measurements were carried out at two different temperatures between the presumed triple point and critical temperature (56 K and 75 K respectively) namely 61.7 and 71.5 K and the results are recalled in table II. Temperatures have been slightly corrected after publication of reference [17] in checking the calibration given by the supplier of our platinum resistance thermometer.

Table II. — *Diffusion coefficient* (*in* 10^{-5} $cm^2.s^{-1}$) *of the saturated* 2D *liquid as a function of coverage for two temperatures. D is coverage independent.*

x	61.7 K	71.5 K
0.30	3.7 ± 0.7	
0.40	4.2 ± 0.5	8.3 ± 0.8
0.55	4.4 ± 0.5	
0.63	4.6 ± 0.5	8.3 ± 0.8

These results are strong evidence that the observed liquid remains the same when x varies. Increasing coverage results only in an extension of the size of the condensed liquid domains. We checked the proportionality of the integrated intensity of the QE peak to the liquid total quantity of adsorbed atoms. This behaviour is a clear proof of the coexistence 2D liquid-gas domain (first order transition) as already stated in reference [17].

3.2.2 *Changing temperature at constant coverage.* — This study has been carried out at $x = 0.63$ in a temperature range from 55 K to 71.5 K. Temperatures are known to ± 0.6 K. The results are shown in figure 5. The line going through error bars is only a guide for eyes. At 57 K, a coexistence of solid and liquid was observed and only the mobility of the

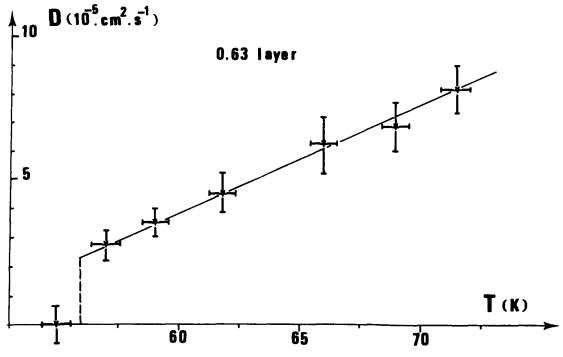

Fig. 5. — Diffusion coefficient *versus* T in the liquid-gas coexistence domain. The full line is a guide to the eye. The sudden drop of the mobility at 56 K indicates a solidification of the layer.

liquid part is taken into account in figure 5. At 55 K the layer is fully solidified (see 3.2.3).

In such a small temperature range, it is always possible to describe the temperature dependence in terms of activation energy. In any case we have to keep in mind that the variation of mobility is not taken along an isochor line but along the coexistence boundary of the L + G domain. Under these assumptions, the activation energy is 24 meV (550 cal./mole) roughly the same as the 2D hypercritical fluid at high coverage.

3.3 SOLIDIFICATION AND LIQUID-SOLID COEXISTENCE. — As recalled in 2.3.2, solidification of a 2D fluid can occur either by decreasing temperature at fixed coverage or by increasing chemical potential i.e. coverage at constant temperature. The two kinds of experiments have been performed here. In the first one, we started with a 0.9 fluid layer at 101.5 K. At 91.5 K, it is still fluid as indicated by the broadening of the quasi-elastic spectra (Fig. 6). However at 76.5 K and below (71.5, 66.5, 61.5 and 55 K), we observe a narrow peak with a width equal to the instrumental resolution which characterizes a solid. Besides, this coverage at low temperature corresponds to the compressed structure [41]. We also observe an intermediate region at 81.5 K where the quasi-elastic spectra (Fig. 6*b*) shows an overall shape which looks like a mixture of curves 6*a* and 6*c*. In fact, the wings of curves 6*b* and 6*c* can be almost superposed up to an intensity about 1 000. This indicates that the 0.9 layer at 81.5 K contains a fluid with nearly the same mobility as at 91.5 K. But curve 6*b* is more peaked than curve 6*c*. We interpret this narrow peak as due to a non negligible quantity of solid. We can notice that a small quantity of immobile phase (~ a few per cent) can be detected by this method since all the intensity scattered by a solid is concentrated near $E = E_0$. This coexistence region between 2D liquid and solid is supported by the previous adsorption isotherm measurements by Thomy and Duval [1] who already interpreted a substep observed around $x = 0.9$ and $T \sim 80$ K as due to a first order transition between a 2D fluid and solid (see paragraph 3.5 for the coverage normalization and the final phase diagram represented in figure 8).

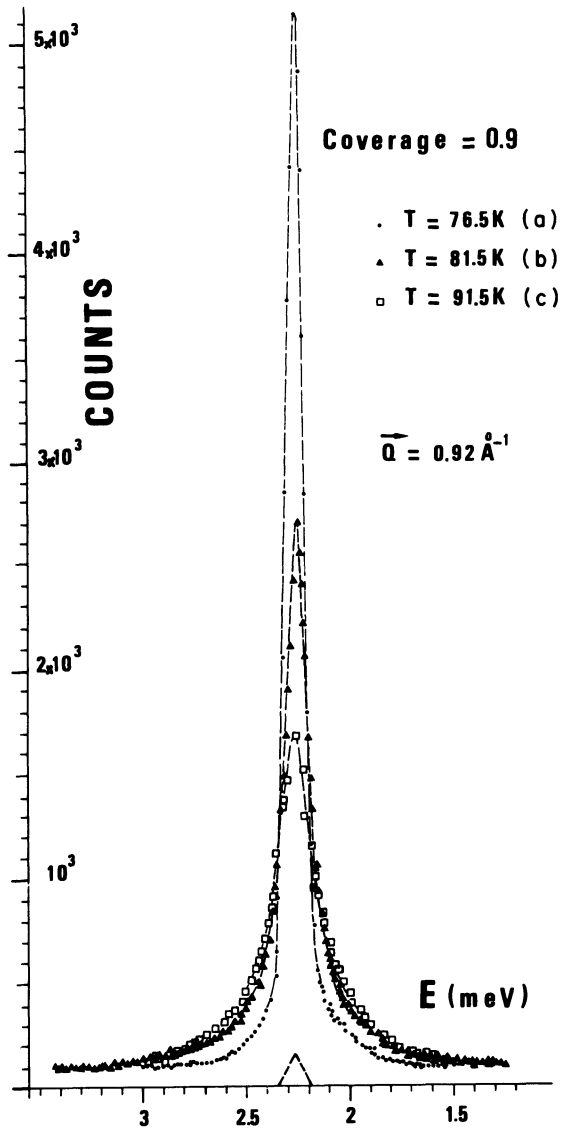

Fig. 6. — Quasi-elastic spectra of a 0.9 layer at three different temperatures. At 76.5 K, the surface film is solidified. At 91.5 K, it is fully melted whereas at 81.5 K the line is due to a mixture of solid and liquid. The dotted lines are guides to the eye.

Another experiment was performed around the triple point (~ 56 K). A 0.63 layer was observed at 59 ± 0.6 K. From paragraph 3.2 we know that in this region 2D gas and liquid coexist. Indeed we measured broad quasi-elastic spectra characteristics of the 2D liquid. At 55 ± 0.6 K the layer is solidified and the scattered line exhibits a narrow shape looking like that in figure 6*a*. At 57 ± 0.6 K the spectra are intermediate between a solid and a liquid shape [53].

The experimental curves suggest the coexistence of solid and liquid in this region. Since solid and liquid can coexist at these low coverages only at the precise temperature of the triple point, the experimental coexistence seems to imply that : *a*) the temperature

varied back and forth over the triple point, or *b*) the system is not ideally uniform.

Finally another experiment was carried out at 91.5 K. Here the coverage was changed ($x = 0.45$; 0.7; 0.9; 1; 1.2). At $x = 0.9$ and below a fluid was observed (3.1). At $x = 1$ and 1.2 the layer was solidified. The narrow spectra due to the solid have been published elsewhere [16].

3.4 ELASTIC INCOHERENT STRUCTURE FACTOR (EISF). — Up to now we did not exploit the non Lorentzian $F(Q)\,e^{-Q^2\langle u^2\rangle}$ terms of equation (1). They represent the product of the incoherent scattering laws due to the rotation and to the vibrations of hydrogen atoms. In the case of methane, for our temperature range, it seems reasonable to use the rotational diffusion model [46]

$$F(Q) = j_0^2(Qa)$$

where a is the gyration radius of the H atoms ($a = 1.09$ Å) and j_0 is the spherical Bessel function of zero order. Since the product $F(Q)\,e^{-Q^2\langle u^2\rangle}$ is almost independent of the preferential orientation of the sample, it can be left out from integration in equation (3). Then the maximum of the observed scattered intensity at $E = E_0$,

$$J_0 = \left| S'(Q, E) \otimes R(Q, E) \right|_{E=E_0}$$

has the following expression for the 2D solid and 2D fluid respectively

$$J_0^s = j_0^2(Qa)\,e^{-Q^2\langle u^2\rangle} \tag{4}$$

$$J_0^f = j_0^2(Qa) \times$$

$$\times\, e^{-Q^2\langle u^2\rangle}\left[\int_0^{2\pi}\int_0^{\pi} \frac{1}{\pi}\,\frac{\hbar DQ^2 \sin^2\tau}{(\hbar DQ^2\sin^2\tau)^2 + (E - E_0)^2}\right.$$

$$\left.\times\, g(\beta)\sin\tau\,d\tau\,d\eta \otimes R(Q, E)\right]_{E=E_0}. \tag{5}$$

The term in brackets of expression (5) is known from the various fits performed in 3 and the two equations can be tested against the experimental results. Figure 7 represents the observed and calculated values of J_0^s and J_0^f as a function of Q^2 for two typical conditions namely $T = 55$ K, $x = 0.9$ in the solid phase and $T = 91.5$ K, $x = 0.9$ in the hypercritical fluid.

The more precise values of J_0 are obtained for the 2D solid because all the intensity is concentrated near $E = E_0$ and the self shielding effect is relatively small. Conversely these two conditions are not fulfilled for the 2D fluid and the uncertainty on J_0^f is larger. The discussion on this latter case will be qualitative only.

Two curves $j_0^2(Qa)$ and $j_0^2(Qa)\,e^{-Q^2\langle u^2\rangle}$ have been calculated to fit J_0^s. The first one has no adjustable parameter (except a normalization factor). Figure 7 shows that it can account for the experimental results

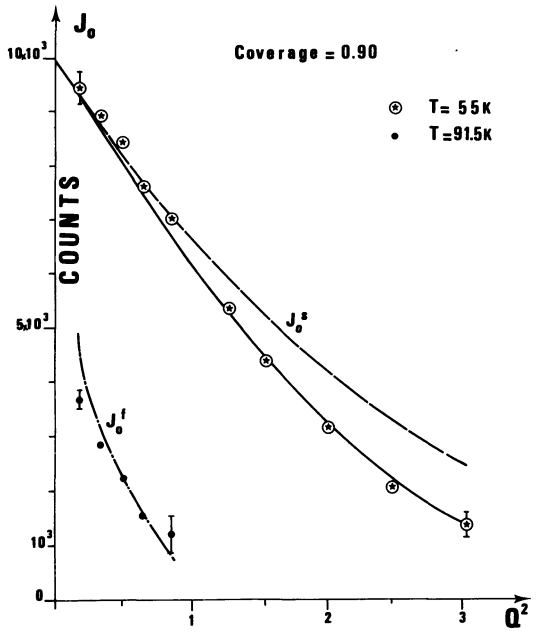

Fig. 7. — Maximum intensity of quasi-elastic spectra *versus* Q^2 in the 2D solid and 2D hypercritical fluid. The calculated curves J_0^s and J_0^f obey equations (4) and (5) respectively (see 3.4). The dashed J_0^s curve has been drawn assuming $e^{-\langle u^2\rangle Q^2} = 1$ whereas the J_0^s full line has been fitted with $\langle u^2 \rangle = 0.062\,5$ Å^{-2}.

below $Q = 1$ Å^{-1}. However the introduction of the Debye-Waller factor is needed at higher Q to fit the observed data. The full line represents the best fit obtained with the adjustable parameter $\langle u^2 \rangle$ equal to 0.062 5 Å^2. This value gives an estimation of the mean square displacement of the hydrogen atoms around their equilibrium position. The good agreement obtained between experiment and theory shows that at 55 K the methane molecules undergo an isotropic rotational diffusion.

As for the spectra maximum J_0^f resulting from the scattering by the 2D fluid, figure 7 shows that equation (5) can account for its variation with Q^2. Due to the uncertainty on the observed J_0^f, it is meaningless to try to adjust $\langle u^2 \rangle$, the only free parameter in (5) and we assume $e^{-Q^2\langle u^2\rangle} = 1$ for the 2D fluid. Here again, the isotropic rotational diffusion model appears to explain the elastic incoherent intensity scattered by the 2D fluid at 91.5 K and $x = 0.9$.

3.5 PHASE DIAGRAM. — All the quasi-elastic experimental results have been summarized in figure 8 in a coverage *versus* temperature diagram. The various observed phases, i.e. the hypercritical fluid, liquid and solid have been noted as well as the points where a mixture of solid and liquid was detected. Other diffraction measurements performed on CD_4/graphite films by the Marseille-Grenoble group have been added [53]. They can define new points in figure 8 where the solid is stable, is melted or coexists with a 2D liquid. In fact two solids have been observed, one registered stable below 47 K and one expanded

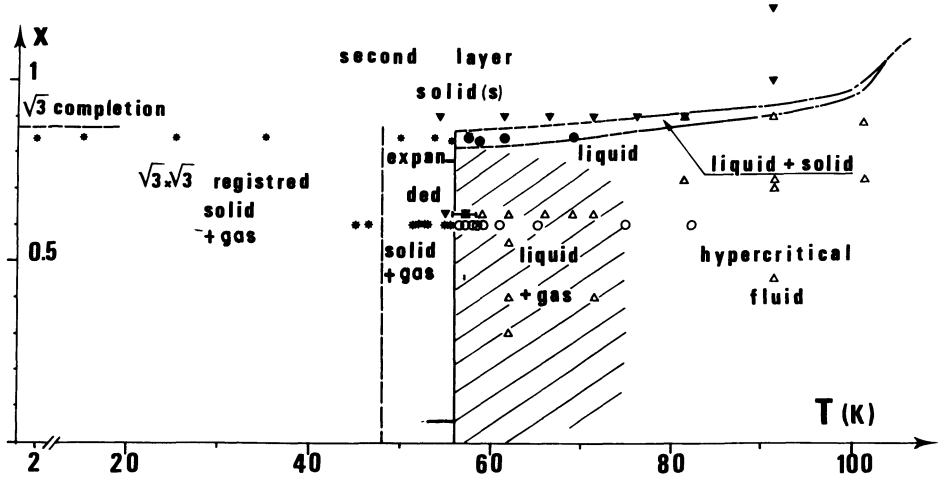

Fig. 8. — Proposed phase diagram of the first layer of methane adsorbed on (0001) graphite. One can notice a triple point at 56 K [13], a critical temperature at about 75 K [1], a solid-solid transition at about 48 K [41, 53] and a narrow liquid-solid coexistence domain. The boundaries of this domain are obtained from this work, from neutron diffraction experiments [13, 53] and from adsorption isotherm measurements ($77 < T < 90$ K-full lines [1]; $90 < T < 106$ K-dash-dotted lines [36]). Quasi-elastic neutron scattering results : ▼ solid, △ fluid. Neutron diffraction results : * solid, ○ fluid. Coverage $x = 1$ corresponds to a molecular density of 0.073 $Å^{-1}$.

occurring between 50 K and 56 K. The transition between the 2 solids is probably continuous (another contracted solid was pointed out by the Oxford and the Argonne groups near the monolayer completion [39, 41]).

We also included the Thomy and Duval liquid-solid coexistence region inferred by adsorption isotherm measurements ($77 < T < 90$ K) [1]. Their coverage has been renormalized against our own coverage definition (at 90 K, $x = 0.9$ corresponds to the beginning of solidification). This obliged us to decrease their film concentration by 3%.

Finally very recent adsorption isotherm results obtained by Terlain, Gilquin and Larher [36] are also reported in figure 8. They extend the phase diagram up to 106.5 K. The liquid-solid coexistence domain ends at about 104 K, a temperature where a line of critical points begins.

All these measurements allow us to propose the phase diagram of the methane submonolayer adsorbed on (0001) graphite. As recalled in the introduction, the triple point (56 ± 0.4 K) was determined previously [13]. The critical temperature was estimated to about 75 K [1]. Between these temperatures, a coexistence domain of 2D liquid and gas occurs but its limits are poorly known. We hatched this region.

On the other hand, the coexistence region between the solid and liquid (stable at higher coverage) is determined more precisely. Above 77 K, the adsorption isotherm measurements by Thomy and Duval [1] and Larher [36] define clearly the limits of this domain. Their results are confirmed by our neutron scattering data at 101.5 K, $x = 0.88$; 91.5 K, $x = 0.9$ and 1.0 and 81.5 K, $x = 0.9$. Below 77 K, we measured a few quasi-elastic spectra at 76.5, 71.5, 66.5, 61.5 and 55 K for a 0.9 layer. As indicated in 3.3, the layer is solidified under these physical conditions. We also measured the diffraction lines of a 0.84 ([1]) layer [53] at 69.2, 61.7, 57.7 K and of a 0.83 layer [13] at 58.7. They show the coexistence of a solid and a liquid. In particular, at 69.2 K, only traces of solid are detected. This permits us to extrapolate the liquid-solid coexistence domain towards the triple point. We also took into account the structural information obtained near the triple point [13, 53] to draw the limits of this region. At melting the mean distance between CH_4 molecules increases by about 2%. Hence the difference in density between the solid and the liquid is about 4% near the triple point.

This phase diagram is qualitatively consistent with that proposed recently by Vora *et al.* [41] if their expanded solid phase S_{II} is actually a mixture of S_{II} plus 2D liquid. The only quantitative disagreement has reference to the value of the triple point we find to be 56 K (Vora *et al.*, 60 K), a temperature which was checked lately against the 2D triple point of N_2 [53]. Upon this assumption and this temperature correction, the position in coverage of the condensed phase boundaries is very close in the two papers. Furthermore, Vora's work brings more structural information near the monolayer completion. Just above the limit of stability of the expanded solid S_{II}, a very narrow existence domain of a $\sqrt{3} \times \sqrt{3}$ registered solid called S_I is observed. The corresponding coverage is $x = 0.87$. Finally, another compressed solid S_{III} is stable between $x = 0.87$ and $x = 1$.

4. **Outlook.** — 4.1 CH_4 SURFACE PHASES. — The mobility of surface films of methane adsorbed on graphite has been measured recently by another nuclear technique, the NMR pulsed field gradient

([1]) The coverage 0.8 given in [53] was actually 0.84.

method that probes molecular motions over times 10^3 larger than the QENS technique. The measurements were performed at one temperature (85 K) for various coverages [37]. The order of magnitude of the diffusion coefficient is the same as ours but the variation of D with coverage is smaller. Furthermore, for coverages greater than one monolayer, the authors did not observe any reduction of the molecular motion consistent with the formation of a solid layer. However, the substrate used in the NMR experiment was some graphitized carbon black (Vulcan III), a powder that is known to have a large specific surface area but poor surface homogeneity. It is reasonable to assume [37] that the difference between the two experiments is mainly due to heterogeneities.

Our results are also worth comparing with the diffusion coefficient in bulk liquid. Its value, a few 10^{-5} cm^2.s^{-1}, in the domain where 3D liquid is stable (above 90 K) is close to our results in two dimensions. This means that the graphite surface field and the reduction in dimensionality do not change drastically the mobility of methane molecules. Besides, we performed another test on the self consistency of our measurements. We filled our experimental cell with bulk liquid at 96 K. The observed diffusion coefficient (2.5×10^{-5} cm^2.s^{-1}) is in agreement with the results obtained by spin echo technique ($D = 3.0 \times 10^{-5}$ cm^2.s^{-1}) [54].

We showed that below 56 K the translational mobility disappeared. Methane molecules are localized at lattice sites. Still they undergo a rotational motion (see § 3.4). At lower temperature, the free rotation of the molecule is partly hindered and methane sits like a tripod on the surface. Below 20 K, several barriers to rotation induce rotational tunnelling transitions that can be observed by neutron scattering spectroscopy [39].

As explained in the introduction, several models have been proposed by theorists to account for the mobility or the phase diagram of methane adsorbed on graphite. We already compared in 3.1 the molecular dynamics simulation by Toxvaerd [26] to our findings. The order of magnitude of the diffusion coefficient at high and medium coverages is retrieved and, of importance, the computation shows that the periodic graphite field does not change appreciably the value of translational mobility. This means that the adsorbed methane fluids have a quasi two-dimensional character.

However at low coverage, all the computer simulations [14, 15, 26] predict a divergence of the 2D diffusion coefficient that is not found in our experiments. Actually, our mobility measurements at $x=0.3$ and 0.45 can be interpreted by the Langevin model of Brownian movement, that is believed to fail at those coverages. This last point should be revisited by theorists.

Other computer simulations have been achieved in the solid stability region [27, 28]. The effect of temperature on the orientational ordering of the CH_4 molecule adsorbed on graphite has been investigated and a transition between a rotationally disordered phase and an ordered structure has been established. One can wonder whether the registered-expanded phase transition around 48 K is related to this orientational ordering. Further neutron measurements are needed to answer the question.

Finally the renormalization group theory has been used to calculate the 2D phase diagram of a triangular lattice gas model which is intended to represent methane physisorbed on basal graphite [25]. A large variety of phase diagrams was obtained depending on the strength of the Lennard-Jones potential which determines the lattice-gas interaction. The general trends of the phase diagram in figure 8 have been found for a given set of interaction parameters but the incommensurate (expanded and contracted) solids do not occur in the calculated results because the lattice gas assumption does not permit anything but localized adsorption.

We think that a more sophisticated model should be proposed to represent the subtle competition between adsorbed molecules and between methane and the periodic graphite field. Then one can expect to account for the stability domains of the various in-registry and out-of-registry CH_4 solids.

4.2 2D MOBILITY. — As shown in this paper, QENS is a good tool to measure the 2D fluid diffusion coefficient and to define clearly the coexistence domain between either 2D liquid and 2D gas or 2D liquid and 2D solid. The hypercritical stability region can also be determined by this technique. Other methods can, in principle, lead to the same results. We already quoted NMR in 4.1. The Mössbauer technique can probe diffusion coefficients inferior or equal to 10^{-8} cm^2.s^{-1}. It has been used to measure the solidification of 2D fluids [22, 55]. Another powerful technique, field emission microscopy, can measure the surface migration in adlayers. It can be employed either on the shadowed field-emission tip mode [56, 57] or on the field-emission fluctuation method [58, 59]. The measurements give valuable information (for instance, tunnelling in surface translational diffusion) about the mobility of molecules adsorbed on the tiny facets of the field emitter metal tip, but the limited size of these facets do not allow one to define true phases in the thermodynamic sense. This limitation is more serious with field ion microscopy which probes individual atoms or molecules and can follow their migration and interaction [60, 61]. Nevertheless this former method can investigate surface atoms with a previously unimaginable sensitivity. It brings a fundamental understanding at the microscopic scale on the surface transport processes and surface reactivity.

This short review shows that strong efforts have been devoted to understand the properties of mobile

atoms or molecules on surfaces. These efforts were successful and surface diffusion is probably one of the best known property of 2D fluids.

Acknowledgments. — We thank Y. Larher for sending us his latest adsorption isotherms of CH_4 on graphite. We thank the IN5's staff for technical assistance.

We acknowledge J. G. Dash and S. C. Fain Jr. for their careful reading of the manuscript and A. J. Dianoux, C. Marti, B. Croset and F. Volino for fruitful discussions.

APPENDIX

In this appendix we first introduce the general formalism of the scattering by a *powder of planes* and indicate how to determine their distribution function $g(\beta)$. Then we apply these general relations to the case of a distribution of 2D liquids and test the obtained scattering law $S'(\mathbf{Q}, E)$ against experimental results achieved for surface films of methane fluid recorded in the in-plane and out-of-plane configurations.

1. **General formalism.** — When a surface phenomenon is probed on a powder sample by a monochromatic and parallel incident beam, the scattered radiation is the sum of the various contributions of the different crystallite surfaces. If all surfaces have the same properties (as those of papyex, a material exhibiting mainly (0001) graphite faces, as explained in 2.1), we can define an angular distribution function $g(\alpha, \beta)$ to describe the quantity of surface for a given orientation. Let us consider a set of reference coordinates $\{ \mathbf{x}_0, \mathbf{y}_0, \mathbf{z}_0 \}$ with $\mathbf{z}_0$ perpendicular to the papyex foil and one particular platlet of the graphite powder defined by the normal $\mathbf{N}_0$ to the basal-plane. The scattering vector $\mathbf{Q}$ makes an angle τ with $\mathbf{N}_0$ and ϕ with $\mathbf{z}_0$. The other angles β, α and η are drawn in figure 9. The probability to find an adsorbing area within the solid angle $d\Omega$ around the direction (α, β) is $g(\alpha, \beta)\, d\Omega$. It describes the angular distribution function of the powder of adsorbing planes. Due to the isotropy of papyex around $\mathbf{z}_0$, this function is in fact independent of α. Its normalization requires

$$\int_0^{\pi} g(\beta) \sin \beta \, d\beta = 1/\pi$$

$g(\beta)$ can be described by a Poisson kernel [62].

It has the advantage of making the following calculations more tractable. Then

$$g(\beta) = \frac{1}{2\pi} \frac{q^{1/2}}{\tanh^{-1} q^{1/2}} \frac{1+q}{(1+q)^2 - 4q\cos^2\beta} \quad (A.1)$$

If an individual surface element gives an elementary effect $I(\mathbf{Q}, E)$, the total contribution of the powder of planes is

$$J(\mathbf{Q}, E) = \int_{\Omega} I(\mathbf{Q}, E)\, g(\beta)\, d\Omega \quad (A.2)$$

where $d\Omega$ is the elementary solid angle around the direction $\mathbf{N}_0$

$$d\Omega = \sin\tau \, d\tau \, d\eta \,. \quad (A.3)$$

Furthermore an elementary relation yields

$$\cos\beta = \sin\phi \cos\eta \sin\tau + \cos\phi \cos\tau \,. \quad (A.4)$$

2. **Determination of $g(\beta)$.** — The above general formulation can be applied to the diffraction of a neutron beam by a powder of planes. It permits us to measure $g(\beta)$. Let us recall that a rocking curve is obtained by recording the variation of the diffracted intensity ($E = E_0$) for a fixed $\mathbf{Q}$ when ϕ varies. Equation (A.2) becomes $J_{\mathbf{Q},E_0}(\phi)$ and $I(\mathbf{Q}, E)$ is constant ($I_{\mathbf{Q},E_0}$).

A rocking curve experiment was performed on the 01 two-dimensional diffracted line of a monolayer of CF_4 adsorbed on graphite. This line is far enough from the 0002 substrate peak and is not perturbed by it. The maximum of the peak was recorded as a function of ϕ. In this geometry $\tau = \pi/2$ and

$$J_{\mathbf{Q},E_0}(\phi) = I_{\mathbf{Q},E_0} \int_0^{\pi} g(\beta)\, d\eta \quad (A.5)$$

where $\beta = \cos^{-1}(\cos\eta \sin\phi)$.

Combining (A.1) and (A.5) yields [62]

$$J_{\mathbf{Q},E_0}(\phi)/I_{\mathbf{Q},E_0} = \int_0^{\pi} g(\beta)\, d\eta$$

$$= \frac{q^{1/2}}{\tanh^{-1} q^{1/2}} [(1+q)^2 - 4q\sin^2\phi]^{-1/2} \,. \quad (A.6)$$

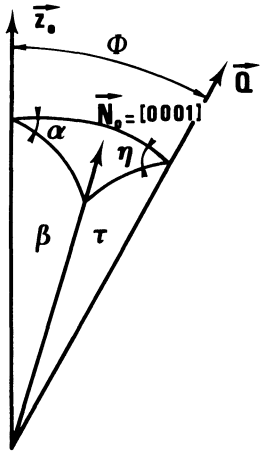

Fig. 9. — Geometrical relationships of $\mathbf{z}_0$ the normal to the foil. $\mathbf{N}_0$ the normal to an individual (0001) surface and $\mathbf{Q}$ the scattering vector.

The experimental results (Fig. 10) can be fitted by (A.6) and the adjustable parameter q can be determined (in our case $q = 0.6$). The function $g(\beta)$ is represented in figure 1.

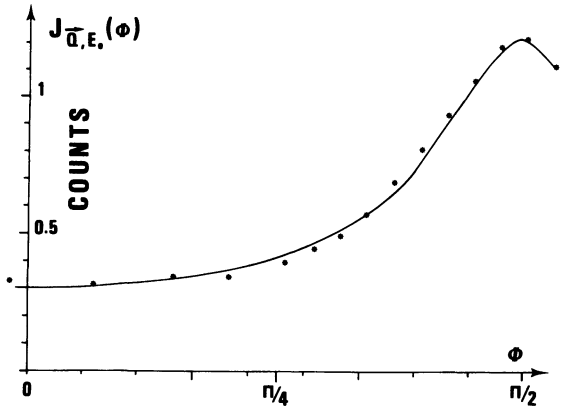

Fig. 10. — Rocking curve of a CF_4 monolayer adsorbed on (0001) graphite. The diffracted intensities have been fitted by equation (A.6) with $q = 0.6$ (full line).

3. **Quasi-elastic scattering by a distribution of 2D liquids.** — The various graphite basal plane of papyex can adsorb 2D fluids whose orientation distribution obeys the $g(\beta)$ law. They interact with neutrons and lead to a broadening of the scattered line. If we assume that the diffusion coefficient is isotropic within the adsorbed layer ($D_{\parallel} = D$) and that the

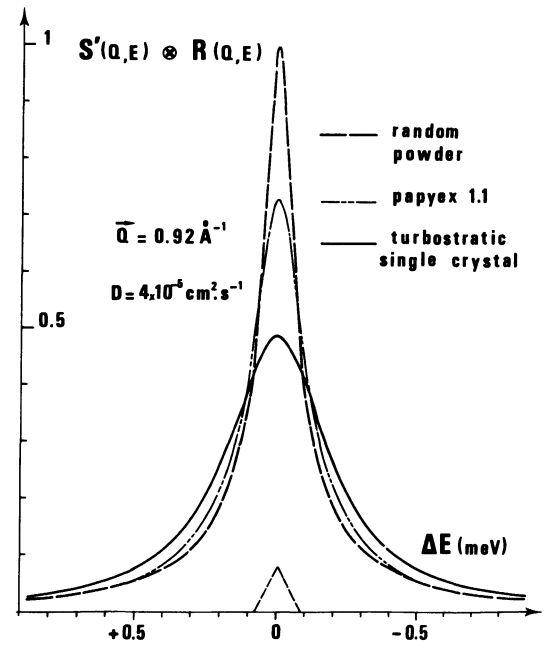

Fig. 11. — Calculated scattering law (equation (3)) convoluted with the instrumental resolution for three different powders in the in-plane geometry (see Fig. 12). If all the surfaces are parallel (turbostractic crystal), the scattering law is Lorentzian (equation (1)). For a randomly oriented powder, the resulting curve is more peaked. For papyex (density 1.1), the line is intermediate between the two extreme situations. Curves have been normalized so that the integrated intensities ($-1 < \Delta E < -1$ meV) are equal.

mobility is restricted within the surface film ($D_{\perp} \simeq 0$), the application of equation (A.2) to quasi-elastic scattering is straight-forward. One must replace $I(\mathbf{Q}, E)$ by the scattering law $S_r(\mathbf{Q}, E)$ (equation (2)). $J(\mathbf{Q}, E)$ becomes $S'(\mathbf{Q}, E)$ and is developed in formula (3).

This expression has been established previously [48, 49] for an isotropic distribution of crystallites ($g(\beta) = 1/2\,\pi$). It appears clearly that the function $S'(\mathbf{Q}, E)$ obtained at fixed Q is no longer a Lorentzian line. $S'(Q, E)$ diverges at $E = E_0$ but when convoluted with the instrumental resolution, the divergence disappears and the resulting function is more peaked than the original Lorentzian curve (see Fig. 11).

4. **In-plane and out-of-plane geometry.** — As explained in introduction, the preferential orientation of papyex can be used to emphasize the motions inside the adsorbed layer. Then the experiment is carried out in the in-plane configuration (Fig. 12*b*). The scattering vector is parallel to the foil ($\phi = \pi/2$). Conversely in an out-of-plane geometry (Fig. 12*a*), the contribution to the scattered intensity of the admolecules motion along the graphite basal planes is reduced. Nevertheless the molecules moving along the misoriented platelets should contribute to the total scattered intensity. Figures 13*a* and 13*b* represent two experiments performed on the same sample at 91.5 K, $x = 0.72$ and $Q^2 = 1.7$ Å^{-2} in the in-plane and out-of-plane geometry respectively. One can see that the two spectra are quite different. The broad peak observed in the in-plane geometry indicates a strong mobility whereas the the narrow line measured in the out-of-plane configuration shows that the mobility perpendicular to the basal plane is very small. As a matter of fact, the wings result from the contribution of misoriented crystallites. Equation (3) accounts for the shape of curves in figure 13. The diffusion coef-

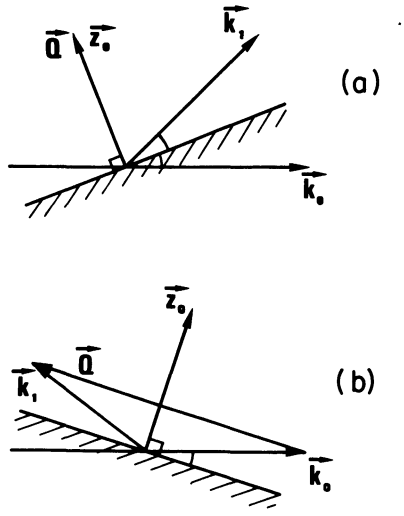

Fig. 12. — In the out-of-plane configuration (Fig. 12*a*), the scattering vector $\mathbf{Q} = \mathbf{k}_0 - \mathbf{k}$, is perpendicular to the foil whereas in the in-plane geometry (Fig. 12*b*) $\mathbf{Q}$ is parallel to it. $\mathbf{k}_0$ and $\mathbf{k}$ are the incident and scattered beams, respectively.

ficient for this physical condition ($x = 0.72$; $T = 91.5$ K) was already measured in a previous experiment (§ 3.1) on a different sample

$$(D = 12 \times 10^{-5}\ \mathrm{cm^2.s^{-1}}).$$

The full lines in figure 13 were calculated using this value of D without any other adjustable parameter, except the maximum intensity of the function. This good agreement between theory and experiment as well as the one obtained in figure 3 show that equation (3) is able to interpret the quasi-elastic scattering by a *powder* of 2D liquids either in the in-plane or out-of-plane geometry.

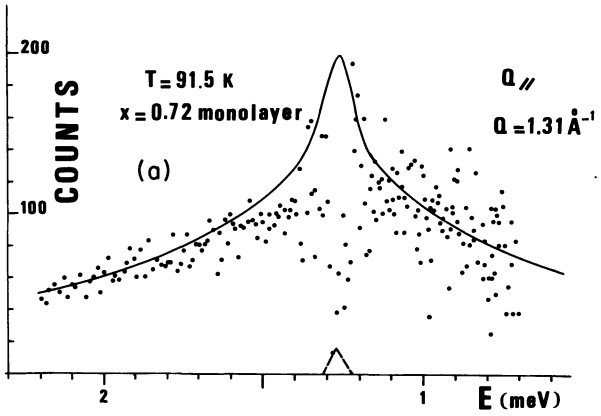

a)

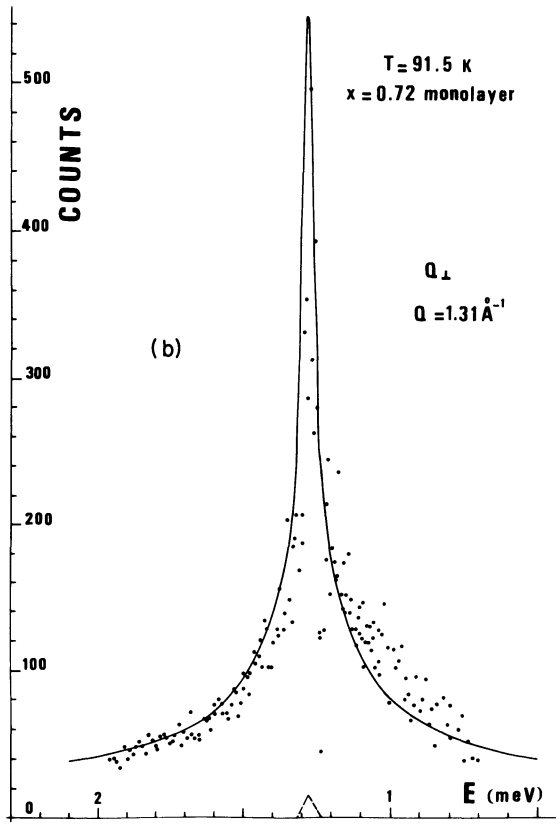

b)

Fig. 13. — An in-plane ($Q_{\|}$, Fig. 13*a*) and out-of-plane experiment ($Q_{\perp}$, Fig. 13*b*). The results have been fitted by equation (3) with the diffusion coefficient obtained in a previous experiment (table I).

References

[1] THOMY, A. and DUVAL, X., *J. Chim. Phys.* **67** (1970) 1101.
[2] DASH, J. G., *Films on solid surfaces* (Acad. Press, N.Y.) 1975.
[3] *Two-dimensional adsorbed phases.* Eds. M. Bienfait et J. Suzanne, *J. Physique Colloq.* **38** (1977) C4.
[4] DASH, J. G., *Phys. Rep.* **38** (1978) 177.
[5] BIENFAIT, M., *Surf. Sci.* **89** (1979) 13.
[6] *Phase transitions in Surface Films*, Eds. J. G. Dash and J. Ruvals (Plenum Press) 1980.
[7] HALPERIN, B. I. and NELSON, D. R., *Phys. Rev. Lett.* **41** (1978) 121 ; *E* **41** (1978) 519.
[8] NELSON, D. R. and HALPERIN, B. I., *Phys. Rev. B* **19** (1979) 2457.
[9] WIDOM, A., OWERS-BRADLEY, J. R. and RICHARDS, M. G., *Phys. Rev. Lett.* **43** (1979) 1340.
[10] HOLZ, A. and MADEIROS, J. T. N., *Phys. Rev. B* **17** (1978) 1161.
[11] ABRAHAM, F. F., *Phys. Rev. Lett.* **44** (1980) 463.
[12] TOXVAERD, S., *Phys. Rev. Lett.* **44** (1980) 1002.
[13] GLACHANT, A., COULOMB, J. P., BIENFAIT, M. and DASH, J. G., *J. Physique Lett.* **40** (1979) L-543.
[14] ALDER, B. J. and WAINWRIGHT, T. E., *Phys. Rev. A* **1** (1970) 18.
[15] POMEAU, Y., *Phys. Rev. A* **5** (1972) 2569.
[16] COULOMB, J. P., BIENFAIT, M. and THOREL, P., in [3], p. 31.
[17] COULOMB, J. P., BIENFAIT, M. and THOREL, P., *Phys. Rev. Lett.* **42** (1979) 733.
[18] RIEHL, J. W. and KOCH, K., *J. Chem. Phys.* **57** (1972) 2199.
[19] ROLLEFSON, R. J., *Phys. Rev. Lett.* **29** (1972) 410.
[20] COWAN, B. P., RICHARDS, M. G., THOMSON, A. L. and MULLIN, W. J., *Phys. Rev. Lett.* **38** (1977) 165.
[21] SATOH, K. and SUGAWARA, T., *J. Phys. Soc. Japan* **46** (1979) 337.
[22] SHECHTER, H., SUZANNE, J. and DASH, J. G., *Phys. Rev. Lett.* **37** (1976) 706.
[23] SCHICK, M., WALKER, J. S. and WORTIS, M., *Phys. Rev. B* **16** (1977) 2205.
[24] SOUTHERN, B. W. and LAVIS, D. A., *J. Phys. C* **12** (1979) 5333.
[25] OSTLUND, S. and BERKER, A. N., *Phys. Rev. B* **21** (1980) 5410.
[26] TOXVAERD, S., *Phys. Rev. Lett.* **43** (1979) 529.
[27] MAKI, K. and NOSE, S., *J. Chem. Phys.* **71** (1979) 1392.
[28] O'SHEA, S. F. and KLEIN, M. L., *J. Chem. Phys.* **71** (1979) 2399.
[29] VENABLES, J. A. and SCHABES-RETCHKIMANN, P., *Surf. Sci.* **71** (1978) 27.
[30] MCTAGUE, J. P. and NOVACO, A. D., *Phys. Rev. B* **19** (1979) 5299.
[31] VILLAIN, J., *Phys. Rev. Lett.* **41** (1978) 36.
[32] VILLAIN, J., *Surf. Sci.* **97** (1980) 219.
[33] TSANG, T., *Phys. Rev. B* **20** (1979) 3497.
[34] FRENKEL, D. and MCTAGUE, J. P., *Phys. Rev. Lett.* **42** (1979) 1632.
[35] LARHER, Y., *J. Chem. Phys.* **68** (1978) 2257.
[36] TERLAIN, GILQUIN and LARHER, Y. to be published.

[37] TABONY, J. and COSGROVE, T., *Chem. Phys. Lett.* **67** (1979) 103.
[38] COULOMB, J. P., KAHN, R. and BIENFAIT, M., *Surf. Sci.* **61** (1976) 291.
[39] NEWBERY, M. W., RAYMENT, R., SMALLEY, M. N., THOMAS, R. K. and WHITE, J. W., *Chem. Phys. Lett.* **59** (1978) 461.
[40] MARLOW, I., THOMAS, R. K., TREVERN, T. D. and WHITE, J. W., in [3], p. 19.
[41] VORA, P., SINHA, S. K. and CRAWFORD, R. K., *Phys. Rev. Lett.* **43** (1979) 704.
[42] SPRINGER, T., *Springer Tracts in Modern Physics*, éd. G. Höhler (Springer Verlag, Berlin) 1972, vol. **64**.
[43] MARSHALL, W. and LOVESEY, S. W., *Theory of thermal neutron scattering* (Clarendon Press, Oxford) 1971.
[44] VAN HOVE, L., *Phys. Rev.* **95** (1954) 249.
[45] VINEYARD, G. H., *Phys. Rev.* **110** (1958) 999.
[46] SEARS, V. F., *Can. J. Phys.* **44** (1966) 1279.
[47] SINGWI, K. S. and SJÖLANDER, A., *Phys. Rev.* **119** (1960) 863.
[48] DIANOUX, A. J., VOLINO, F. and HERVET, H., *Mol. Phys.* **30** (1975) 1181.
[49] STOCKMEYER, R., *Ber. Bunsenges. Phys. Chem.* **80** (1976) 625.
[50] COULOMB, J. P., BIENFAIT, M. and THOREL, P., *Proc. 7th Intern. Vac. Congr. and 3rd Intern. Conf. Solid Surfaces*, Vienna, R. Dobrozemsky ed. 1977, vol. **II**, p. 1337.
[51] BOATO, G., CANTINI, P. and TATAREK, R., *Phys. Rev. Lett.* **40** (1978) 887.
[52] GLASSTONE, S., LAIDLER, K. J. and EYRING, H., *The theory of rate processes* (McGraw-Hill Book Company N.Y.) 1941, p. 486.
[53] GLACHANT, A., COULOMB, J. P., BIENFAIT, M., THOREL, P., MARTI, C. and DASH, J. G., *Proceedings of the International Conference on « Ordering in Two Dimensions »*, S. K. Sinha ed. (Elsevier North-Holland Publ. Co), to be published.
[54] OOSTING, P. H. and TRAPPENIERS, N. J., *Physica* **51** (1971) 418.
[55] SHECHTER, H., SUZANNE, J. and DASH, J. G., *J. Physique* **40** (1979) 467.
[56] GOMER, R., *Disc. Faraday Soc.* **28** (1959) 23.
[57] GOMER, R., *Field Emission and Field Ionization* (Harvard Univ. Press, Cambridge) 1961, chap. 4.
[58] GOMER, R., *Chemistry and Physics of Solid Surfaces*, R. Vanselow ed. (CRC Press, Boca Raton) 1979, Vol. **II**, p. 423.
[59] DI FOGGIO, R. and GOMER, R., *Phys. Rev. Lett.* **44** (1980) 1258.
[60] TSONG, T. T. and COWAN, P. L., *Chemistry and Physics of Solid Surfaces*, R. Vanselow ed. (CRC Press, Boca Raton) 1979, Vol. **II**, p. 209.
[61] WRIGLEY, J. D. and EHRLICH, G., *Phys. Rev. Lett.* **44** (1980) 661.
[62] RULAND, W. and TOMPA, H., *Acta Crystallogr.* **A 24** (1968) 93.